

DOI: 10.5281/zenodo.2640031
CZU 621.833:519.8



MATHEMATICAL MODELLING OF TEETH CONTACT IN PRECESSIONAL TRANSMISSION

Viorel Bostan¹, Ion Bostan², Maxim Vaculenco^{3*}, Mihail Țopa⁴

¹Technical University of Moldova (TUM), Department of "Soft Engineering and Applied Mathematics",

²TUM, Department of "Machine Projecting Basics", Republic of Moldova

³TUM, Department of "Industrial and Product Design", Republic of Moldova

⁴TUM, Department of "Physics", Republic of Moldova

*Corresponding Author: Maxim Vaculenco, maxim.vaculenco@dip.utm.md

Received: March, 09, 2019

Accepted: March, 23, 2019

Abstract. The article deals with the development of the $2K-H$ precessional toothed gear with convex-concave contact of the teeth. The teeth flanks of the satellite are described in the circular arc, and the central wheels - with convex / concave profiles.

The article addresses issues of increasing the convex-concave contact load bearing capacity by identifying the conjugated profiles with the small difference in the curvature radius. The design of the contact takes into account the decrease of the friction sliding between the conjugated flanks in view of the increase of the mechanical efficiency of the transmission.

The synthesis of the toothed precessional gear is based on the study of the kinematics of the contact point and of the rational co-ratio of the conjugated flanks curvature radii . The geometry of the teeth contact is analyzed according to the parametric configuration $[Z_g-\theta;\pm 1]$ and is modified by concrete technical solutions aiming at increasing the load bearing capacity and energy efficiency of the contact.

The paper describes: the new processes basic principles of the teeth generation by spatial rotation and rolling, which allow the manufacture of conical toothed wheels with varying convex/concave profile of the teeth.

Keywords: *precessional transmissions, convex-concave contact, kinematics of the contact point, generation of teeth with varying convex/concave profile.*

1. Introduction

The ever-growing demands of mechanical transmission consumers on increasing the transmission power, mass and size reduction, etc., can be met on two developmental directions, namely by creating new types of mechanical transmissions based on new operating principles and/or by increasing the bearing capacity of the gear teeth contact, for example of the convex-concave contact researched in the works [1, 2, 3].

Precessional transmissions with multiple gear, invented in 1981, have developed both in terms of improving the new mechanism of movement transformation as well as the performance or contact geometry of the gear teeth, which over time have been protected by over 180 patents.

Figure 1 shows the submersible precessional garmotor for actuating the robot

displacement mechanism on the ocean floor of the Robotic Complex¹ for the extraction of ferro-manganese (CFM) concretions from deep depths (4...7 km)² [4].

The $2K-H$ type submersible reducer developed based on the precessional transmission with a gear with bolts (TPB) is made up of four nodes elements: crank shaft 1, satellite 2 with two teeth of conical bolts, installed floating on the crank shaft 1, between the fixed 3 and mobile 4 general wheels. The difference in number of teeth and conjugated bolts is ± 1 . When rotating the crank shaft 1, the satellite 2 in its spherical-spatial motion engages its crowns in the bolts with the teeth of the fixed 3 and mobile 4 central wheel, thus ensuring the reduction of the rotation movement with the transmission ratio in the range $i=\pm 10... \pm 3600$. To compensate for hydrostatic pressures $P=40\div 70$ MPa the gearmotor is equipped with the compensators 7.

Precessional transmissions have also developed in terms of performance of the teeth contact geometry.

Figure 2 shows the electromechanical module for the operation of the space flight technique³, developed based on $2K-H$ type precessional transmission with convex-concave contact of the gear teeth. The electromodule is characterized by high kinematic precision $\psi'' = 60''$ angular sec., with a relatively small starting moment $T=320$ gcm with pre-tightening in the gearing, high torsional stiffness $\varphi=1.5\cdot 10^5$ Nm/rd [4].

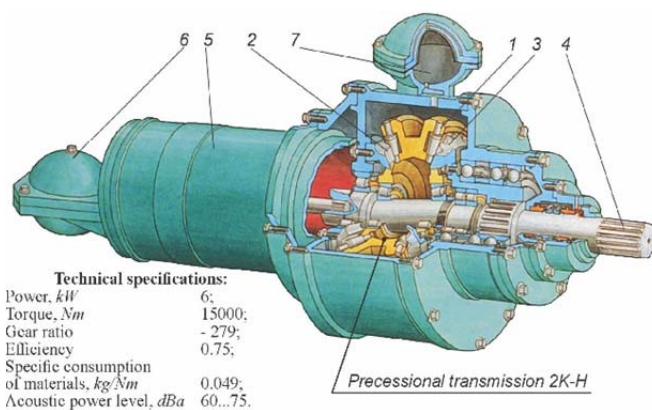


Figure 1. Precessional submersible gearmotor with bolt gear, $i=-279$.

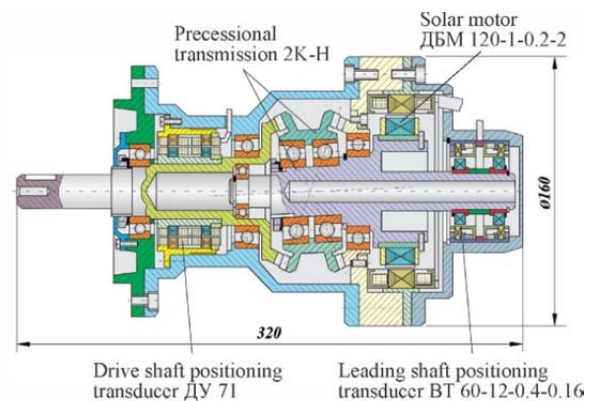


Figure 2. Precessional electromechanical module with toothed gear ($i=-279$) for the operation of the space flight technique.

Remark 1: TPB and TPD Precessional Transmissions do not have analogues among the world-wide known transmissions regarding the broad range of transmission reports, including kinematic possibilities to operate under reductor, multiplier, and differential regime.

2. Advantages and disadvantages of TPB and TPD

Compared to evolving transmissions, TPB is characterized by disadvantages like:

1. The bearing capacity of the "conical tooth-bolt" contact is limited by the radius of curvature of the conical bolts.
2. The crowns of the satellite made of conical bolts make it irrational, difficult, sometimes impossible to manufacture gears with diameters of less than 50 mm, which limits their extension to kinematic actuators (robots, fine mechanics, technological equipment, etc.).

¹ State Secret with the initial "Top Secret".

² Only in the Pacific Ocean, more than 1700 billion tons of CFM are located.

³ State Secret with the initial "Top Secret".

3. Considering the condition of the similarity of the shape of the conical bolts in the real transmission to the teeth generating tool, at their small diameters, the productivity of teeth generation decreases and the manufacturing costs increase.

4. In order to ensure the cutting speed, the technological process of generating the small diameter of the tool requires a considerable increase of its rotational speed, and the rigidity of the system and the precision of execution decrease.

These drawbacks of the precessional transmission with “conical tooth-bolt” gearing (TPB) can be elucidated by the development of precessional transmissions with toothed gear (TPD).

A first step in the assertion of precessional transmissions with toothed gear is the invention patent “Precessional gear transmission” [4] later developed in [5]. The precessional transmission gear shown in figure 3, (a), (b), (c) is conical consisting of a satellite-wheel with circular arc-shaped teeth with the origin of the radius of curvature R located on the normal $n-n$ raised from the point of contact of the teeth conjugated (see figure 3, (a), (b), (c)). The radius of curvature R of the arc-shaped profile may be increased by up to 7 radii r of the circumference entered into the thickness of the arc-shaped profile tooth.

Figure 3 (d), (e), (f) shows the profilograms of the central wheel teeth Z_1 described by $\zeta=f(\xi)$ correlated with the trajectory of the movement of the origin of the radius of curvature of the teeth profile of the satellite Z_2 in the arc of the circle $\zeta_1=f(\xi_1)$. The profilograms obtained for different parametric configurations $[Z_g-\theta;\pm 1]$ of the gear. The load bearing capacity of the gears with convex-concave contact of the teeth can be increased by decreasing the difference of the curvature radius of the conjugate profiles.

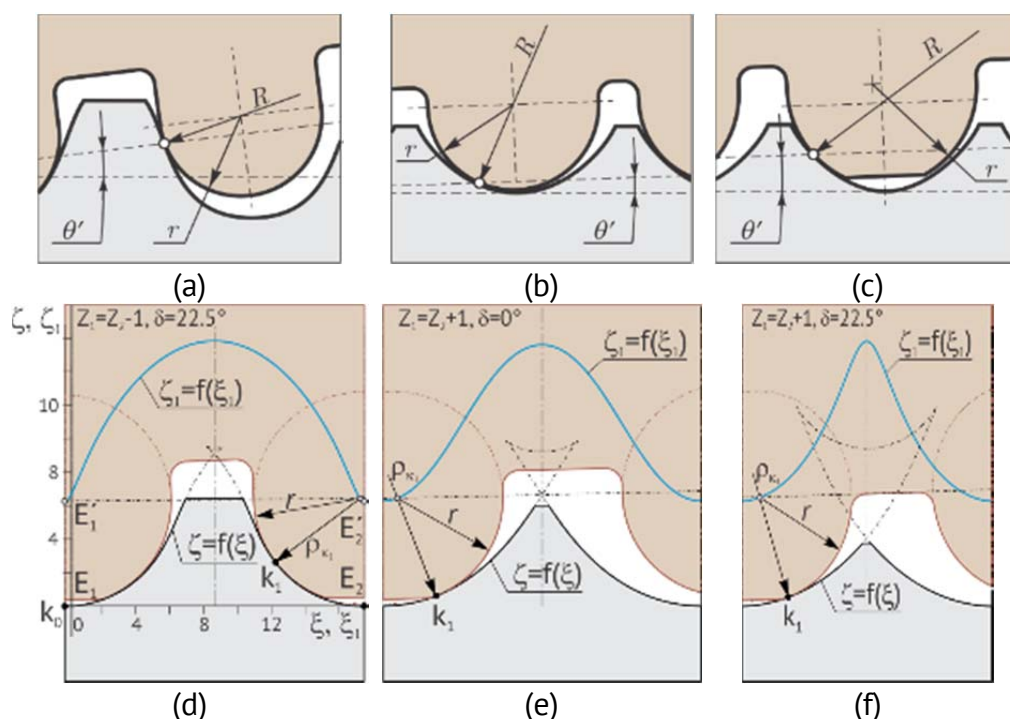


Figure 3. Geometry of teeth contact in the toothed precessional gear: a, b, c – contact with the profile of the teeth in the circular arc and convex / concave; d, e, f – convex-concave contact with small difference of the curvature radii of conjugated profiles for different parametric configurations $[Z_g-\theta;\pm 1]$.

The transformation of the movement and the transmission of the load in the precession gear takes place by rolling with the presence of sliding between the conjugate flanks. Rolling is a function of the angle of the nutation and the sliding between the flanks depends on the parametric configuration $[Z_g-\theta;\pm 1]$ of the gear. The presence of sliding leads to a reduction in the mechanical efficiency of the gear, to tightening restrictions on the physical and mechanical properties of the wheel material, to imposing costly constructive and exploitation solutions.

Remark 2: The load-bearing capacity and the mechanical efficiency of the TPD are still two important objectives for research and development of precessional transmissions, which will be addressed in terms of transforming the geometry of the teeth contact.

3. Synthesis of the precessional toothed gear with convex-concave contact

To create the convex-concave contact of the teeth engaged in spherical-space movement we admit that the profile of the teeth of the satellite (see figure 4) are designated by the curve LEM of radius r . In the figure 4, $\zeta_1=f(\xi_1)$ shows the trajectory of the movement of the origin of the radius r in the sphero-spatial movement of the satellite, and the function $\zeta=f(\xi)$ represents the profile of the teeth of the central wheels described by the flank wrap of the satellite teeth with the arbitrary profile LEM.

From the Euler kinematic equations, taking into account the kinematic relation between the angles φ and ψ expressed by $\varphi = -Z_1\psi/Z_2$, we get the trajectory of the movement LEM $\zeta_1=f(\xi_1)$ of the origin G of the radius of the circular arcs expressed by the coordinates X_G, Y_G, Z_G depending on the crank shaft rotation angle ψ :

$$\begin{aligned} X_G &= R \cos \delta \left[-\cos \psi \sin(Z_1\psi/Z_2) + \sin \psi \cos(Z_1\psi/Z_2) \cos \theta \right] - R \sin \delta \sin \psi \sin \theta, \\ Y_G &= -R \cos \delta \left[\sin \psi \sin(Z_1\psi/Z_2) + \cos \psi \cos(Z_1\psi/Z_2) \cos \theta \right] + R \sin \delta \cos \psi \sin \theta, \\ Z_G &= -R \cos \delta \cos(Z_1\psi/Z_2) \sin \theta - R \sin \delta \cos \theta. \end{aligned} \tag{1}$$

where θ is the angle of the nutation;
 δ – the angle of the conical axoid.

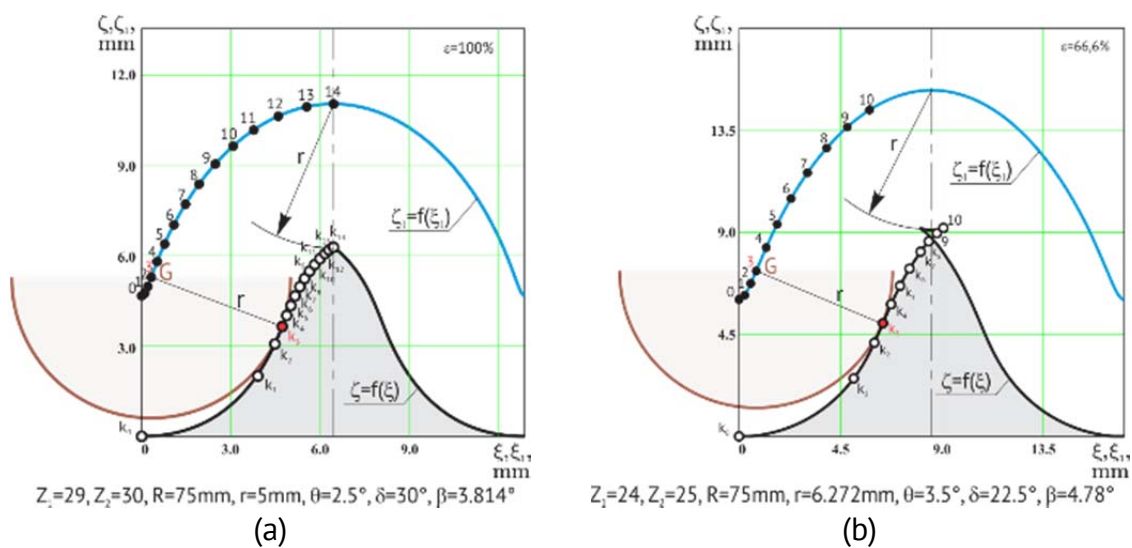


Figure 4. Active contact of the teeth in in the precessional gear with frontal reference multiplicity $\varepsilon = 100\%$ (a) and $\varepsilon = 66.6\%$ (b).

We determine the equation of the wrap of the circular arcs family LEM on the sphere of the radius R by jointly solving the equations describing the surfaces of the satellite teeth flanks with circular arc profile [5]

$$\Phi(X, Y, Z, \psi) = X\bar{X}_G + Y\bar{Y}_G + Z\bar{Z}_G - Rr \cos \beta = 0$$

$$\frac{d\Phi}{d\psi}(X, Y, Z, \psi) = 0 \quad 2$$

and the equation of the sphere surface

$$X^2 + Y^2 + Z^2 - R^2 = 0 \quad 3$$

For this, from the equations (2) and (3) we write

$$\frac{d\Phi}{d\psi} = X \frac{\partial \bar{X}_G}{\partial \psi} + Y \frac{\partial \bar{Y}_G}{\partial \psi} + Z \frac{\partial \bar{Z}_G}{\partial \psi},$$

$$\frac{\partial \bar{X}_G}{\partial \psi} = \frac{\partial X_G}{\partial \psi} \cos \psi_3 - \frac{X_G}{u} \sin \psi_3 + \frac{\partial Y_G}{\partial \psi} \sin \psi_3 + \frac{Y_G}{u} \cos \psi_3,$$

$$\frac{\partial \bar{Y}_G}{\partial \psi} = -\frac{\partial X_G}{\partial \psi} \sin \psi_3 - \frac{X_G}{u} \cos \psi_3 + \frac{\partial Y_G}{\partial \psi} \cos \psi_3 - \frac{Y_G}{u} \sin \psi_3,$$

$$\frac{\partial \bar{Z}_G}{\partial \psi} = \frac{\partial Z_G}{\partial \psi}.$$

$$\frac{\partial X_G}{\partial \psi} = -R \cos \delta (1 - \cos \theta) \cos 2\psi - R \sin \delta \sin \theta \cos \psi,$$

$$\frac{\partial Y_G}{\partial \psi} = -R \cos \delta (1 - \cos \theta) \sin 2\psi - R \sin \delta \sin \theta \sin \psi, \quad 4$$

$$\frac{\partial Z_G}{\partial \psi} = +R \cos \delta \sin \theta \sin \psi.$$

where $\psi_3 = \psi / u$ is the angle of rotation of the blank, u – the transmission ratio of the kinematic chain *main axis - blank*, $\bar{X}_G, \bar{Y}_G, \bar{Z}_G$ – the coordinates of the G origin of the radius of curvature of the tool in the coordinate mobile system $O\bar{X}_1\bar{Y}_1\bar{Z}_1$, Z_G, Y_G, X_G – the coordinates of the G origin of the radius of curvature of the tool in the fixed coordinate system $OXYZ$ [4];

After replacing (4) in (2) and (3) we obtain

$$X_0 = \frac{-(ab + de) \pm \sqrt{(ab + de)^2 + (1 + a^2 + d^2)(R^2 - b^2 - e^2)}}{1 + a^2 + d^2},$$

$$Y_0 = aX_0 + b,$$

$$Z_0 = dX_0 + e. \quad 5$$

where,

$$a = \left(\bar{X}_G \frac{\partial \bar{Z}_G}{\partial \psi} - \bar{Z}_G \frac{\partial \bar{X}_G}{\partial \psi} \right) / \left(\bar{Z}_G \frac{\partial \bar{Y}_G}{\partial \psi} - \bar{Y}_G \frac{\partial \bar{Z}_G}{\partial \psi} \right),$$

$$b = \left(-R^2 \cos \beta \frac{\partial \bar{Z}_G}{\partial \psi} \right) / \left(\bar{Z}_G \frac{\partial \bar{Y}_G}{\partial \psi} - \bar{Y}_G \frac{\partial \bar{Z}_G}{\partial \psi} \right),$$

$$d = -\frac{(\bar{X}_G - a\bar{Y}_G)}{\bar{Z}_G}, \quad e = \frac{R^2 \cos \beta - b\bar{Y}_G}{\bar{Z}_G}.$$

Equations (5) describe the wrap of the circular arcs family on the sphere and represent the teeth profile of the central wheels. In order to represent the teeth profile of the central wheels in the normal section we project the wrap on the sphere on a P_1 plane and after a series of transformations we obtain the projection into the plane of the profile of the central wheel teeth defined by the Cartesian coordinates:

$$\xi = \frac{(E_1 E_2) + (X - X_1)^2 + (Y - Y_1)^2 + (Z - Z_1)^2}{2E_1 E_2} - \frac{(X - X_2)^2 + (Y - Y_2)^2 + (Z - Z_2)^2}{2E_1 E}, \quad 6$$

$$\zeta = \sqrt{(X - X_1)^2 + (Y - Y_1)^2 + (Z - Z_1)^2 - \xi^2}.$$

Remark 3: Based on the formation principle of the wrap of the circular arcs family (5) with the origins located on the curve $\zeta_1=f(\xi_1)$ there was developed the generation model through spatial rotation and rolling of the teeth of the central wheel, which reproduces the geometry and kinematics of the teeth interaction in the real precessional transmission.

4. Precessional convex-concave contact with transformable geometry

Position of the origins of the circular arcs G_2 located on the curve $\zeta_1=f(\xi_1)$ presented in figure 4 by p. 1,2,3 ... i correspond to the precession angles ψ of the crank shaft rising from one pair of teeth to the other with the angular step $\psi = 2\pi \cdot Z_2 / Z_1^2$.

Depending on the precession phase ψ of the satellite, each pair of teeth of the conjugated wheels "satellite - central wheel" passes through three geometrical shapes of contact. In the points k_0, k_1 and k_2 located in the foot area of the teeth of the central wheel the contact is convex-concave, in the points k_3 and k_4 - convex-rectilinear, and in the contacts $k_5... k_{14}$ (figure 4, (a)) and $k_5... k_8$ (figure 4, (b)) the contact is convex-convex.

The radius of curvature at a certain point i of the teeth profile of the central wheel is calculated according to the formula

$$\rho_i = \sqrt{(X_i - X_{ci})^2 + (Y_i - Y_{ci})^2 + (Z_i - Z_{ci})^2} \quad 7$$

in which X_{ci}, Y_{ci}, Z_{ci} are the coordinates of the center of curvature c_i

$$X_{ci} = \frac{\Delta_{1i}}{\Delta_i}, \quad Y_{ci} = \frac{\Delta_{2i}}{\Delta_i}, \quad Z_{ci} = \frac{\Delta_{3i}}{\Delta_i}. \quad 8$$

where $\Delta_i, \Delta_{1i}, \Delta_{2i}$ and Δ_{3i} are the determinants of the equation system

$$\begin{aligned} \Delta_i &= \Delta X_i (c_i \Delta Y_{i+1} - b_i \cdot \Delta Z_{i+1}) + \\ &+ \Delta Y_i (a_i \cdot \Delta Z_{i+1} - c_i \cdot \Delta X_{i-1}) + \\ &+ \Delta Z_i (b_i \cdot \Delta X_{i+1} - a_i \cdot \Delta Y_{i+1}), \end{aligned} \quad 9$$

$$\Delta_{1i} = d_i (\Delta Y_i \cdot \Delta Z_{i+1} - \Delta Y_{i+1} \cdot \Delta Z_i), \quad 10$$

$$\Delta_{2i} = d_i (\Delta Z_i \cdot \Delta X_{i+1} - \Delta Z_{i+1} \cdot \Delta X_i), \quad 11$$

$$\Delta_{3i} = d_i (\Delta X_i \cdot \Delta Y_{i+1} - \Delta X_{i+1} \cdot \Delta Y_i). \quad 12$$

Figure 5 shows the variation of the difference of the curvature radius ($\rho_{ki} - r$) of the teeth profile of the central wheel ρ_{ki} and of the teeth of the satellite with the radius r in the

contacts k_i of the conjugated flanks, depending on the precession angle ψ for the toothed gears with different parametric configuration $[Z_g-\theta;\pm 1]$.

The profiles of the teeth flanks of the central wheel are described by the function $\zeta=f(\xi)$ built according to the parametric equations of the wrapping of the circular arcs of the radius r with the origin located on the trajectory of its movement $\zeta_1=f(\xi_1)$. The profile of the satellite teeth is prescribed by a curve in circular arc with the origin of the curvature radii located on the same curve $\zeta_1=f(\xi_1)$.

It is obvious that the bearing capacity of the gear increases if the geometry of the teeth contact has the convex-concave shape, and based on the classical theory of teeth contact as deformable bodies, the difference in radii of curvature of the conjugated flank profiles tends to be minimal. This criterion in precessional transmissions with toothed gear is achievable by two interdependent solutions:

1. By varying the configuration parameters $[Z_g-\theta;\pm 1]$, which determines the shape of the teeth profile of the central wheel;
2. By excluding from the gear the pair of teeth with convex-convex and/or convex-rectilinear geometric contact, thus extending the contact area of the teeth with convex-concave geometry.

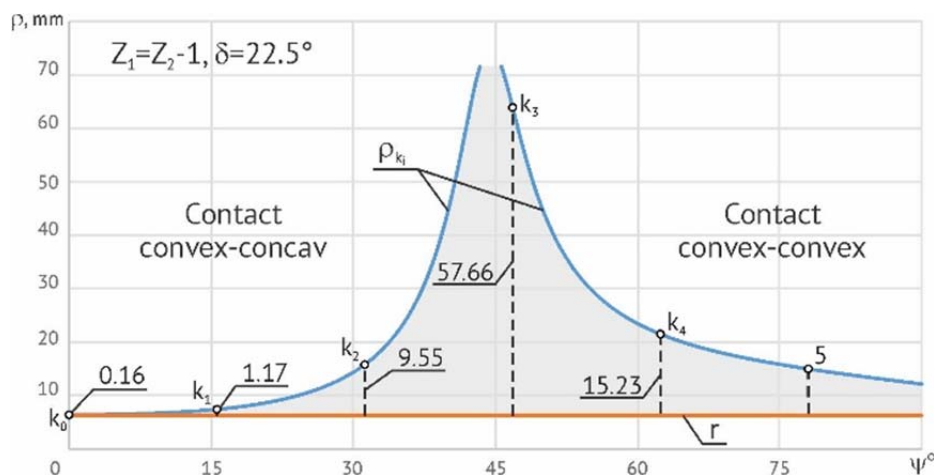


Figure 5. The difference of the curvature radii ($\rho_{k_i}-r$) of the teeth profiles of the central wheel ρ and of the satellite r in the contact k_i depending on ψ for $Z_1=Z_2-1$ and $\delta=22.5^\circ$ ($Z_1=24, Z_2=25, \theta=3.5^\circ, \delta=22.5^\circ, r=6.27\text{ mm}, R=75\text{ mm}$).

By multifactorial analysis of equations (2) - (6) and according to the condition of the fundamental law of the gearing to ensure the constant transmission ratio, the modification of the shape of the implicit teeth profiles and the performance characteristics of the convex-concave contact of the conjugated flanks was argued.

5. Precessional convex-concave contact with low friction sliding between the flanks

Another important criterion for designing the geometry of the precessional toothed contact is to minimize or exclude the relative friction sliding between the conjugated flanks, which leads to an increase in the mechanical efficiency of the transmission

Based on these considerations there are determined the linear speeds of the teeth contact point E separate for the point E_1 which belongs to the tooth profile of the central wheel and for E_2 which belongs to the tooth profile of the satellite.

The position vector of the contact point of the conjugated teeth, which belongs to the tooth profile of the central wheel E_1 is identified by the following vector equation.

$$\vec{r}_{E_1} = \vec{r}_{G_2} + \overline{G_2E_1} = \vec{r}_{G_2} + \vec{r} \quad 13$$

in which, $\overline{G_2E_1} = \vec{r} = R \sin \beta \frac{\vec{v}_{G_2} \times \vec{r}_{G_2}}{|\vec{v}_{G_2} \times \vec{r}_{G_2}|}$ and $\vec{r}_{G_2} = \vec{r}_G \cdot \cos \beta$, where: \vec{r} – the position vector of

the point E_1 against point G_2 has the module equal to the curvature radius of the satellite teeth profile with circular arc profile;

\vec{r}_G and \vec{r}_{G_2} – are the position vectors of the origin of the curvature radius of the satellite teeth, respectively, both located on the directrix GO (see figure 6).

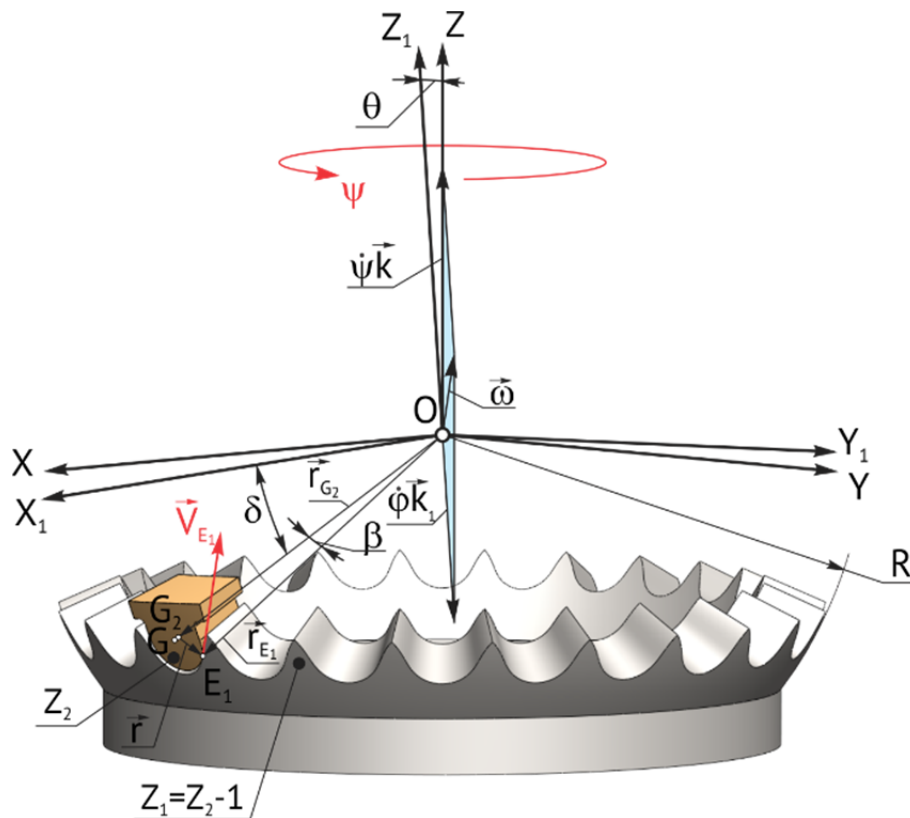


Figure 6. Vector diagram of vector positioning of contact point speeds V_{E_1} and V_{E_2} on the tooth profile of the central wheel and the satellite.

The position vector of the origin of the curvature radius \vec{r}_{G_2} can be expressed by the coordinates X_{G_2} , Y_{G_2} , Z_{G_2} , thus

$$\begin{aligned} \vec{r}_{E_1} &= \vec{r}_{G_2} + \overline{G_2E_1} = \vec{r}_{G_2} + \vec{r}, \\ \vec{r}_{G_2} &= x_{G_2} \cdot \vec{i} + y_{G_2} \cdot \vec{j} + z_{G_2} \cdot \vec{k}, \\ \dot{\vec{r}}_{G_2} &= \dot{x}_{G_2} \cdot \vec{i} + \dot{y}_{G_2} \cdot \vec{j} + \dot{z}_{G_2} \cdot \vec{k}. \end{aligned} \quad 14$$

The motion trajectory on the radius sphere R of the origin of the curvature radius r of the teeth profile G (X_G , Y_G , Z_G) of the satellite depending on the angle ψ , in the fixed coordinates system $OXYZ$ is determined from relations:

$$\begin{aligned} X_G &= R \cdot \cos \delta (-\cos \psi \sin \varphi_\psi + \sin \psi \cos \varphi_\psi \cos \theta) - R \cdot \sin \delta \sin \psi \cdot \sin \theta, \\ X_G &= R \cdot \cos \delta (-\cos \psi \sin \varphi_\psi + \sin \psi \cos \varphi_\psi \cos \theta) - R \cdot \sin \delta \sin \psi \cdot \sin \theta, \\ Z_G &= -R \cdot \cos \delta \cos \varphi_\psi \cdot \sin \theta - R \cdot \sin \delta \cos \theta. \end{aligned} \quad 15$$

The projections of the vector \vec{v}_{E_1} on the axes X, Y, Z is determined by the expressions:

$$\begin{aligned} V_{E_1X} &= \dot{x}_{G_2} + \frac{R \sin \beta}{\left(\sqrt{a_x^2 + a_y^2 + a_z^2}\right)^3} \left[(a_x^2 + a_y^2 + a_z^2) \dot{a}_x - (a_x \dot{a}_x + a_y \dot{a}_y + a_z \dot{a}_z) a_x \right]; \\ V_{E_1Y} &= \dot{y}_{G_2} + \frac{R \sin \beta}{\left(\sqrt{a_x^2 + a_y^2 + a_z^2}\right)^3} \left[(a_x^2 + a_y^2 + a_z^2) \dot{a}_y - (a_x \dot{a}_x + a_y \dot{a}_y + a_z \dot{a}_z) a_y \right]; \\ V_{E_1Z} &= \dot{z}_{G_2} + \frac{R \sin \beta}{\left(\sqrt{a_x^2 + a_y^2 + a_z^2}\right)^3} \left[(a_x^2 + a_y^2 + a_z^2) \dot{a}_z - (a_x \dot{a}_x + a_y \dot{a}_y + a_z \dot{a}_z) a_z \right]. \end{aligned} \quad 16$$

and the module of the contact point speed E_1 depending on the precession angle ψ is determined by the relation

$$V_{E_1} = \sqrt{V_{E_1X}^2 + V_{E_1Y}^2 + V_{E_1Z}^2} \quad 17$$

The positioning of the speed vector of the contact point E_2 , which belongs to the tooth profile of the satellite wheel according to the vectorial diagram figure 6, can be represented by:

$$\overline{r}_{E_1} = \overline{OE_1} = \overline{OE_2} = \overline{r}_{E_2},$$

where,

$$\begin{aligned} \overline{OE_1} &= x_{E_1} \vec{i} + y_{E_1} \vec{j} + z_{E_1} \vec{k}, \\ \overline{OE_2} &= x_{1E_2} \vec{i}_1 + y_{1E_2} \vec{j}_1 + z_{1E_2} \vec{k}_1. \end{aligned} \quad 18$$

To determine the coordinates of the contact point E_2 we express the position of the satellite through the versors $\vec{i}_1, \vec{j}_1, \vec{k}_1$ depending on the versors $\vec{i}, \vec{j}, \vec{k}$ and Euler angles ψ, θ, φ :

$$\begin{aligned} x_{1E_2} &= (x_{E_1} \vec{i} + y_{E_1} \vec{j} + z_{E_1} \vec{k}) \cdot \vec{i}_1, \\ y_{1E_2} &= (x_{E_1} \vec{i} + y_{E_1} \vec{j} + z_{E_1} \vec{k}) \cdot \vec{j}_1, \\ z_{1E_2} &= (x_{E_1} \vec{i} + y_{E_1} \vec{j} + z_{E_1} \vec{k}) \cdot \vec{k}_1. \end{aligned}$$

Analogously to p. E_1 to calculate the speed of the contact point E_2 we determine the module of the contact point speed E_2 on the satellite tooth profile according to the relation

$$V_{E_2} = \sqrt{\dot{x}_{1E_2}^2 + \dot{y}_{1E_2}^2 + \dot{z}_{1E_2}^2} \quad 19$$

where,

$$\begin{aligned} \dot{x}_{1E_2} = V_{E_2X_1} = V_{G_2X_1} &+ \frac{R \sin \beta}{\left(\sqrt{a_x^2 + a_y^2 + a_z^2}\right)^3} \times \left\{ (a_x^2 + a_y^2 + a_z^2) \dot{a}_x - (a_x \dot{a}_x + a_y \dot{a}_y + a_z \dot{a}_z) a_x \right\}; \\ \dot{y}_{1E_2} = V_{E_2Y_1} = V_{G_2Y_1} &+ \frac{R \sin \beta}{\left(\sqrt{a_x^2 + a_y^2 + a_z^2}\right)^3} \times \left\{ (a_x^2 + a_y^2 + a_z^2) \dot{a}_y - (a_x \dot{a}_x + a_y \dot{a}_y + a_z \dot{a}_z) a_y \right\}; \\ \dot{z}_{1E_2} = V_{E_2Z_1} = V_{G_2Z_1} &+ \frac{R \sin \beta}{\left(\sqrt{a_x^2 + a_y^2 + a_z^2}\right)^3} \times \left\{ (a_x^2 + a_y^2 + a_z^2) \dot{a}_z - (a_x \dot{a}_x + a_y \dot{a}_y + a_z \dot{a}_z) a_z \right\}. \end{aligned} \quad 20$$

Knowing the variation of the linear speeds of the contact points E_1 and E_2 , it is determined the variation of the relative sliding speed between the teeth flanks depending

on the angle ψ , $V_{al(\psi)} = V_{E_1(\psi)} - V_{E_2(\psi)}$, presented in figure 9 for the precessional gear with the co-ratio of the number of teeth $Z_1=Z_2-1$ (see figure 3, (d)).

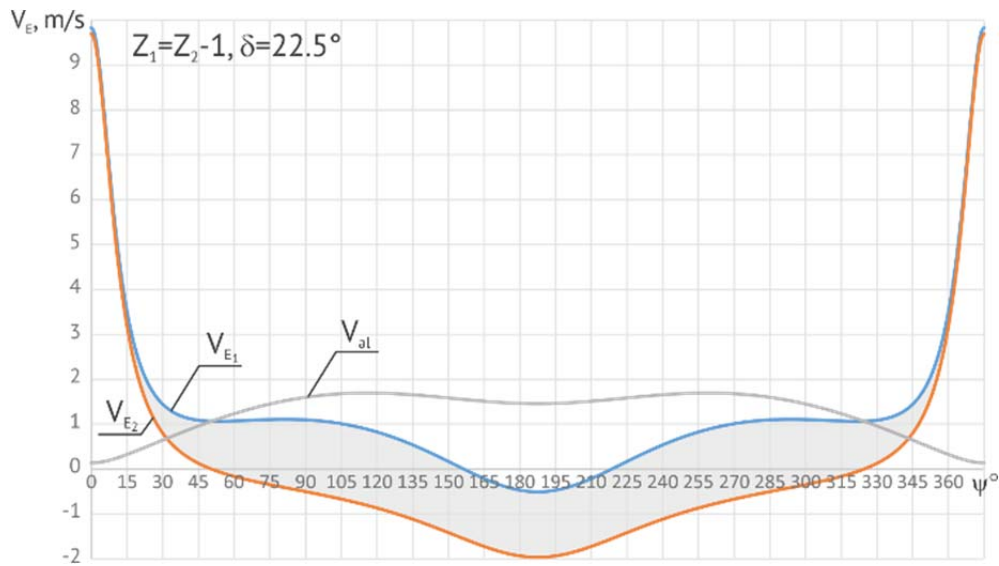


Figure 7. The relative sliding speed V_{al} between the teeth flanks depending on the angle ψ , for $Z_1=Z_2-1$ (precessional gear $Z_1=24$, $Z_2=25$, $\theta=3.5^\circ$, $\delta=22.5^\circ$, $\beta=4.78^\circ$, $r=6.27$ mm, $R=75$ mm).

Also, there were analyzed the variations in linear speeds at the contact point of the teeth V_{E_1} and V_{E_2} and their difference $V_{al} = V_{E_1} - V_{E_2}$ for the gears:

- figure 3, (e) with the co-ratio of the number of teeth $Z_1=Z_2+1$ and the angle of the conical axoid $\delta=22.5^\circ$;
- figure 3, (f) with the co-ratio of the number of teeth $Z_1=Z_2+1$ and the angle of the conical axoid $\delta=0^\circ$.

6. Kinematics and geometry of the convex-concave precession contact

The kinematics of the contact point of the teeth in precessional gear and the geometrical shape of the conjugated flanks represent two determinant characteristics of mechanical efficiency and bearing capacity of the contact.

The mechanical efficiency of the gear is the expression of the energy losses generated by the frictional forces with sliding between the conjugated flanks and the bearing capacity of the convex-concave contact depends on the difference in size of the radii of curvature thereof.

For these reasons, contact kinematics and geometry are examined for gears with parametric configurations $[Z_g-\theta;\pm 1]$ that are different among them only through the co-rotation of the teeth number $Z_1=Z_2\pm 1$ and the angle of the conical axoid $\delta \geq 0^\circ$. Taking the above into account, the generalized parametric configuration can be expressed by $Z_1=24(25)$, $Z_2=25(24)$, $\theta=3,5^\circ$, $\delta=22,5^\circ(0^\circ)$, $r=6,27$ mm and $R=75$ mm.

The kinematics of the contact points $k_0, k_1, k_2 \dots k_i$ corresponding to the crank shaft positioning angles $\psi_0, \psi_1, \psi_2 \dots \psi_i$ is characterized by varying the linear speeds V_{E_1} and V_{E_2} and the relative sliding speed between the flanks $V_{al_{k_i}}$. The geometry of the teeth contact in the points $k_0, k_1, k_2 \dots k_i$ is characterized by the radii of curvature ρ_{k_i} and r of the conjugated profiles and their difference $(\rho_{k_i}-r)$. The analysis of the kinetics of the teeth contact is performed for the frequency of the revolutions of the crank shaft $n_1=3000$ min^{-1} .

Thus, for the gearing corresponding to the configuration $[Z_g-\theta;-1]$ with the co-ratio of the teeth numbers $Z_1=Z_2-1$ and the angle of the conical axoid $\delta=22.5^\circ$ presented in figure 8, (a) the linear speed in the teeth contact k_0 $V_{E_1} = 9.83m/s$, $V_{al_{k_0}} = 0.14m/s$, and the curvature radius of the teeth profile of the central wheel $\rho_{k_0} = 6.43mm$ of the satellite wheel $r=6.27mm$ and their difference $\rho_{k_0} - r = 0.16mm$ (see figure 8, (b)).

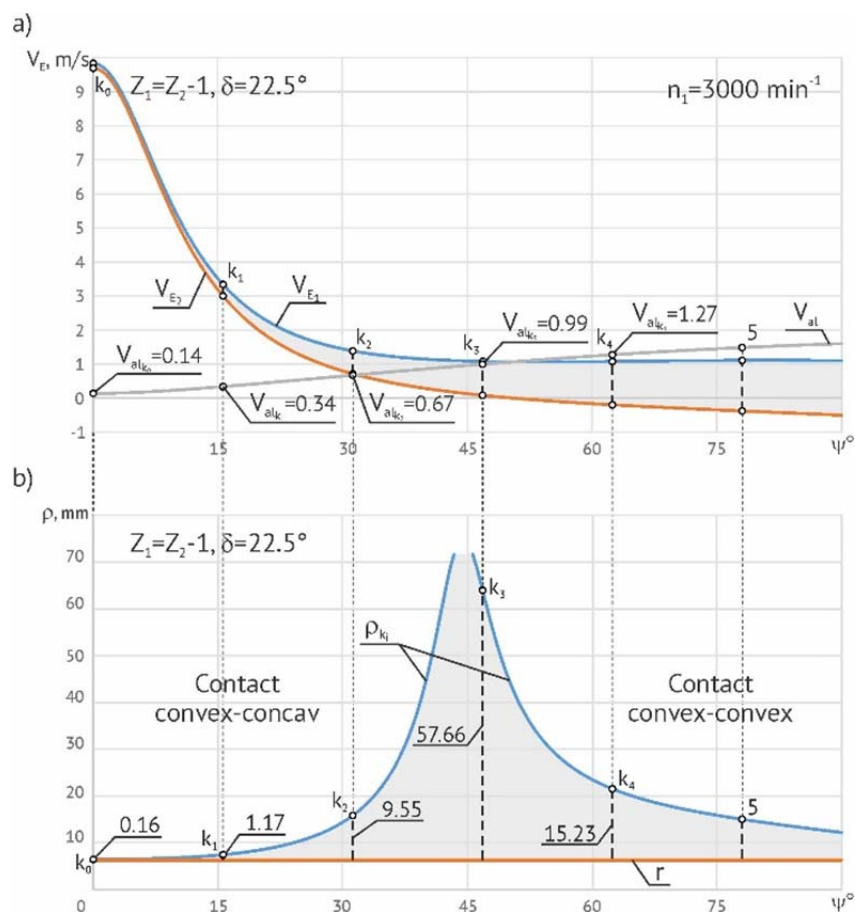


Figure 8. The linear speeds at the contact point, V_{E_2}, V_{E_3} (a) and the difference in curvature radii $(\rho_{k_i} - r)$ (b) of the conjugated profiles in the contact k_i depending on ψ for $Z_1=Z_2-1$ and $\delta=22,5^\circ$ ($Z_1=24, Z_2=25, \theta=3,5^\circ, \delta=22.5^\circ, r=6.27 \text{ mm}, R=75 \text{ mm}$).

With the increase of the angular coordinate from one conjugated pair to the other with the step $\psi = 2\pi i Z_2 / Z_1^2$ for example: from the angular coordinate $\psi_{k_0} = 0^\circ$ up to $\psi_{k_1} = 15.6^\circ$ attributed to contact k_1 the linear speeds V_{E_1} and V_{E_2} decreases k_1 registering in contact k_1 the difference $V_{al_{k_1}} = V_{E_1 k_1} - V_{E_2 k_1} = 0.34m/s$ and the difference of the curvature radii of the conjugated flanks in k_1 $\rho_{k_1} - r = 1.17mm$; in contact k_2 corresponding to $\psi_{k_2} = 31.2^\circ$, $V_{al_{k_2}} = 0.67m/s$ and the difference of the curvature radii $\rho_{k_2} - r = 9.55mm$; in contact k_3 , corresponding to $\psi_{k_3} = 46.8^\circ$ $V_{al_{k_3}} = 0.99m/s$, and the geometry of the teeth contact passes from convex-concave to convex-convex with the external curvature radius of the teeth profile of the central wheel $\rho_{k_3} = 57.66mm$.

The analysis of the gearing with parametric configuration $[Z_g-\theta;+1]$, the co-ratio of the number of teeth $Z_1=Z_2+1$ (recommended for multipliers) and the angle of the conical

axoid $\delta=22.5^\circ$ showed that in the contact of the teeth flank k_0 the relative sliding speed $V_{al_{k_0}} = 1.57 \text{ m/s}$ and the difference of the curvature radii $\rho_{k_0} - r = 4.53 \text{ mm}$; in k_1 corresponding to $\psi_{k_1} = 13.8^\circ$ $V_{al_{k_1}} = 1.59 \text{ m/s}$ and $\rho_{k_1} - r = 4.91 \text{ mm}$; in k_2 corresponding to $\psi_{k_2} = 27.6^\circ$ $V_{al_{k_2}} = 1.65 \text{ m/s}$ and $\rho_{k_2} - r = 5.96 \text{ mm}$ and in k_3 corresponding to $\psi_{k_3} = 41.4^\circ$ $V_{al_{k_3}} = 1.71 \text{ m/s}$ and $\rho_{k_3} - r = 7.73 \text{ mm}$.

From the perspective of the research on the wear of the convex-concave contact of the teeth it is necessary to analyze in complex the relative sliding speed V_{al} between the teeth flanks and the distances $S_1(\psi)$ and $S_2(\psi)$ made by the contact points E_1 and E_2 , respectively, on the teeth profiles of the central wheel and of the satellite depending on the precession angle ψ . The distances traveled by the contact point on the teeth profiles of the central wheel S_1 and satellite wheel S_2 are considered equal to the distance traveled between the positions determined by the angles $\psi_{k_0} = 0$ and $\psi_{k_i} = 360 \cdot i \cdot Z_2 / Z_1^2$, where $i=1,2,3,\dots$ - the order number of the conjugated teeth pairs (see figure 4).

Taking into account the above, the distance traveled by the contact point E_1 on the teeth flank of the central wheel is determined by the formula

$$S_1(\psi) = \int_0^{\frac{Z_2\psi}{Z_1}} \sqrt{\left(\frac{dx_{E_1}}{d\psi}\right)^2 + \left(\frac{dy_{E_1}}{d\psi}\right)^2 + \left(\frac{dz_{E_1}}{d\psi}\right)^2} d\psi = \int_0^t \sqrt{\dot{x}_{E_1}^2 + \dot{y}_{E_1}^2 + \dot{z}_{E_1}^2} dt \quad 21$$

where, $\dot{x}_{E_1}, \dot{y}_{E_1}$ and \dot{z}_{E_1} are the projections of the speed vector of the point E_1 \vec{V}_{E_1} on the axes X, Y and Z .

The distance traveled by the contact point in E_2 on the profile of the teeth flank of the satellite wheel in circular arc for the same values of the precession angle ψ is determined by the formula:

$$S_2(\psi) = \int_0^{\frac{Z_2\psi}{Z_1}} \sqrt{\left(\frac{dx_{1E_2}}{d\psi}\right)^2 + \left(\frac{dy_{1E_2}}{d\psi}\right)^2 + \left(\frac{dz_{1E_2}}{d\psi}\right)^2} d\psi = \int_0^t \sqrt{\dot{x}_{1E_2}^2 + \dot{y}_{1E_2}^2 + \dot{z}_{1E_2}^2} dt \quad 22$$

where, $\dot{x}_{1E_2}, \dot{y}_{1E_2}, \dot{z}_{1E_2}$ are the projections of the speed vector of the point E_2 on the coordinate axes x_1, y_1, z_1 .

The distance $S_1(\psi)$ and $S_2(\psi)$ traveled, respectively, by the point E_1 on the tooth flank of the central wheel (21) and by the point E_2 on the tooth flank of the satellite wheel (22) in relation to time (or the precession angle ψ) are defined by the integral $\int_0^t V_E dt$ and can be calculated according to Simpson's formula

$$\int_a^b f(x) dx \approx \frac{b-a}{3n} [y_0 + (y_1 + y_3 + y_5 + \dots + y_{n-1})4 + (y_2 + y_4 + y_6 + \dots + y_{n-2})2 + y_n] \quad 23$$

where, n - even number, $y_0 = f(x_0) = f(a)$; $y_i = f(x_i)$; $y_n = f(x_n) = f(b)$

For example, the distance traveled by point E_1 on the tooth flank of the central wheel S_1 in relation to time or the precession angle ψ will be:

$$S_1(t) = \int_0^t v_{E_1} dt = \int_0^t \sqrt{(\dot{x}_{E_1})^2 + (\dot{y}_{E_1})^2 + (\dot{z}_{E_1})^2} dt = \int_0^\psi \sqrt{\left(\frac{dx_{E_1}}{d\psi}\right)^2 + \left(\frac{dy_{E_1}}{d\psi}\right)^2 + \left(\frac{dz_{E_1}}{d\psi}\right)^2} d\psi = \int_0^\psi \Phi(\psi) d\psi \quad 24$$

or in accordance with Simpson's formula $S_1(\psi)$ it is

$$S_1(\psi) \cong \frac{\psi - \psi_0}{3 \cdot i} [\Phi(0) + (\Phi_1 + \Phi_3 + \Phi_5 + \dots + \Phi_{i-1})4 + (\Phi_2 + \Phi_4 + \Phi_6 + \dots + \Phi_{i-2})2 + \Phi_i] \quad 25$$

Analogously, substituting in the formula (24) V_{E_1} with V_{E_2} we obtain the distance $S_2(i)$ traveled by the point E_2 on the tooth flank of the satellite wheel depending on the precession angle ψ .

The difference in the distances covered by the points E_1 and E_2 between their common contact, for instance, in k_0 , corresponding to the precession angle $\psi=0$ and their position when $\psi = \psi_i$ represents the relative sliding between the teeth flanks of the conjugated wheels, thus

$$V_{sl} = \Delta S = S_1(\psi) - S_2(\psi).$$

In figure 9 it is presented the variation of distances S_1 and S_2 traveled by the points E_1 and E_2 between the positions defined with the angles ψ_{k_0} and ψ_{k_i} corresponding to the contacts $k_0 \dots k_i$ of pairs of simultaneously engaged teeth and their difference ΔS for the toothed precessional gearing with the parameters $Z_1=24, Z_2=25, \theta=3.5^\circ, \delta=22.5^\circ, r=6.27 \text{ mm}$ and $R=75 \text{ mm}$.

In figure 9, (a) there are presented the distances traveled S_1 and S_2 and their difference ΔS from the teeth contact k_0 ($\psi = 0$) and up to each teeth contacts $k_1 \dots k_4$, only for the first four pairs of bearing teeth conjugated as a result of the modification of the shape of the teeth profile of the central wheel (that transmits the load), and in figure 9, (b) it is presented the location topology on the teeth profiles of the central and satellite wheel of the contact points $E_i^{(1)}$ and $E_i^{(2)}$ for the same values of the precession angle ψ .

From the analysis in figure 9, (a) it can be observed that between the teeth contacts k_0 and k_1 corresponding to the angles $\psi=0$ and $\psi_{k_1} \cong \frac{2\pi i Z_2}{Z_1} = 15,6^\circ$ the difference in the distances S_1-S_2 made by the contact points E_1 and E_2 is only 0.17 mm , between the contacts k_0 and k_2 the difference in the distances covered is $\Delta S=0.57 \text{ mm}$, between the contacts k_0 and k_3 $\Delta S=1.25 \text{ mm}$, between k_0 and k_4 - $\Delta S=2.17 \text{ mm}$, between k_0 and k_5 $\Delta S=3.29 \text{ mm}$, between k_0 and k_6 $\Delta S=4.57 \text{ mm}$, between k_0 and k_7 $\Delta S=5.94$, and between k_0 and k_8 $\Delta S=7.35 \text{ mm}$.

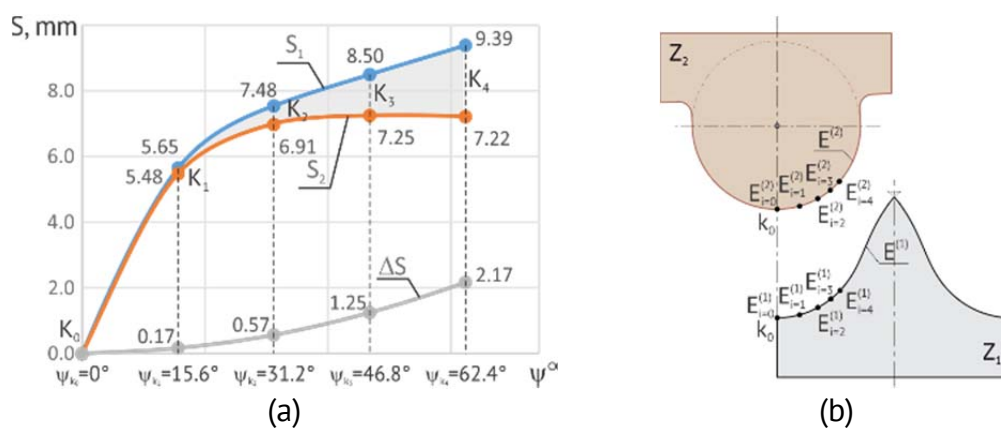


Figure 9. Distances S_1 and S_2 traveled by the contact points E_1 and E_2 between positions with ψ_{k_0} and ψ_{k_8} and their difference ΔS for the gear with the modified shape of the teeth (a) and the location topology on the profiles of the similar contact points $E_i^{(1)}$ and $E_i^{(2)}$ (b) (precessional gear $Z_1=24, Z_2=25, \theta=3.5^\circ, \delta=22.5^\circ, \beta=4.78^\circ, r=6.27, R=75 \text{ mm}$).

In order to diminish the relative sliding in the contact and, respectively, to increase the mechanical efficiency of the gear, the teeth geometry of the central wheel and satellite S is modified so that the difference in distances traveled ΔS by the contact points E_1 and E_2 is decreased. The difference in the distances traveled by the contact points E_1 and E_2 is an important kinematic feature for the development of the tribological model of the teeth contact.

For these reasons, by changing the shape of the central wheel teeth, we exclude the teeth contacts from the gear ($k_5 \dots k_8$) with a big difference ΔS in the distances covered by the contact points E_1 and E_2 . Thus, in the gear, we keep only the contacts $k_0 \dots k_4$ with a small difference in the distances covered ΔS , to mention, with convex-concave geometry favorable to the increase of the contact carrier (see figure 9).

Remark 4: *The analysis of the gear kinematics and of the geometry of the conjugated flanks contact in the same angular coordinates of the precession phase ψ , allows the overall estimation of the mechanical efficiency and the bearing capacity of the contact, also allows the identification of favorable contact geometry for ensuring the optimum lubrication and of the criteria for developing the tribological model of the contact.*

7. Teeth generation by spatial rotation and rolling with convex-concave profiles and in circular arc

The generation process of the teeth of central wheels in precessional gears basically is based on the reproduction of the interaction of the teeth of the satellite wheel with the profile in circular arc with the teeth of the central wheel, and on respecting the kinematics in real precessional transmission.

To generate the teeth of the central wheel with convex / concave profile, there have been developed three technological processes, distinguished by the geometry of the tool and the shape of the contour generating it.

In the elaborated procedures [10], the tool in the shape of a truncated cone, a peripheral profiled disk or cylindrical, performs sphero-spatial motion with the trajectory of the movement of the center of the generator contour described in the $OXYZ$ immobile coordinate system with the equations:

$$\begin{aligned} X_D &= -R_u \cos \delta (1 - \cos \Theta) \cos \varphi \sin \varphi - R_u \sin \delta \sin \Theta \sin \varphi; \\ Y_D &= -R_u \cos \delta (\sin^2 \varphi + \cos \Theta \cos \varphi) + R_u \sin \delta \sin \Theta \cos \varphi; \\ Z_D &= -R_u \cos \delta \sin \Theta \cos \varphi - R_u \sin \delta \cos \Theta. \end{aligned} \quad 26$$

The profile of the teeth flanks of the central wheel is materialized by the wrap of the contours generating family of the tool, determined by the equations of the generating surface, for example of the tool in the shape of a truncated cone and by its relative movement parameters of the tooth in the winding.

To simplify the determination of the wrap of the contours generating family it is passed to the coordinates of the center D of the tool in the mobile coordinate system, linked to the blank:

$$\begin{aligned} \overline{X}_D &= X_D \cos \psi_3 + Y_D \sin \psi_3; \\ \overline{Y}_D &= -X_D \sin \psi_3 + Y_D \cos \psi_3; \\ \overline{Z}_D &= Z_D. \end{aligned} \quad 27$$

where $\overline{X_D}, \overline{Y_D}, \overline{Z_D}$ are the coordinates of the tool center in the mobile system of coordinates; $\psi_3 = \psi/i$ is the rotation angle of the blank; i – the transmission ratio of the kinematic chain *main axis – blank*. The equations (27) determine the movement trajectory of the center of the tool, deployed on the sphere.

The teeth profile of the central wheel (blank) generated by spatial rotation and rolling basically represents the positioning wrap depending on ψ of the generating contours of the tool of the radius r projected on the sphere of the radius R described by the equations (2)...(5). **The generation procedure by spatial rotation and rolling with precessional tool in the shape of a “truncated cone”**. According to the procedure the tool performs the sphero-spatial movement round the fixed point O , has the geometrical shape of a truncated cone and reproduces the geometry and sizes of the bolt in the real precessional transmission with bolts [10].

Figure 10, (a) shows the tooth profile shaping scheme of the central wheel through the generation procedure with spatial rotation and rolling. To describe the evolving formation of the imaginary tooth profile we analyze the interaction of the generating contour of the tool with the processed tooth, in different phases of formation, respecting the condition $\omega_H/\omega_b = const.$, where ω_H and ω_b are the angular speeds, respectively the main axis H of the machine-tool and the blank b . Thus, when rotating the main axis H with the angle $\varphi_H = 360^\circ/16$, the processed tooth moves from position 1 to position 2. The peripheral part of the tool processes the tooth profile in the point 2'' when its center is in the point 2''. The process is then repeated. At a rotation of the main axis, the peripheral part of the tool carries out the continuous processing of a tooth while the center of the tool will describe the trajectory 1'', 2'', 3''...16''.

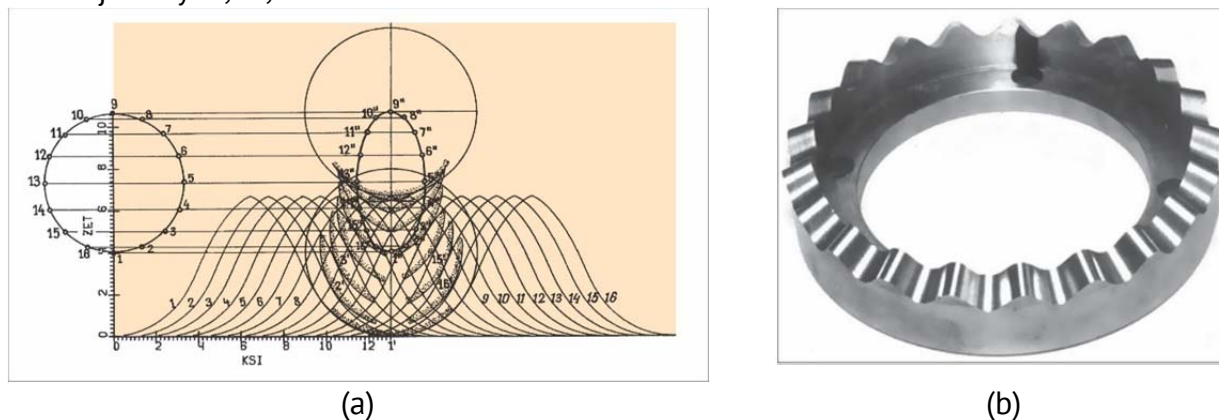


Figure 10. The position scheme of generation by spatial rotation and rolling of the teeth of conical wheels, with the precessional tool in the shape of truncated cone (a) and samples of manufactured toothed wheels (b, c).

Figure 17 (b) present the immobile central wheels with convex/concave profile of the teeth generated by spatial rotation and rolling with the tool in the shape of truncated cone.

To achieve the generation procedure by spatial rotation and rolling of the teeth with convex-concave and variable profile, the construction of the tool holder device for teeth generation has been developed according to the positioning scheme of the tool-blank in figure 10, (a). The process summarizes the following: the tool (milling cutter or grinding stone in the geometrical shape of a truncated cone) is communicated with a series of

coordinated movements with respect to the rotating blank. The kinematic connection of the blank with the tool ensures the rotation of the blank with a tooth at a closed cycle of the spatial movement communicated to the tool. The tool is assigned the kinematic link between the „tool-frame of the machine-tool” respecting the function between the position rotation angle of the tool φ and the rotation angle of the main axis ψ , $\varphi = -\arctg(\cos\theta \operatorname{tg}\psi)$.

In this case, through the process there may be generated a variety of convex / concave profiles, including with longitudinal and profile modification.

Using the rolling kinematic chain of the tool-machine to grind the tool and the blank are brought into a coordinated movement of spatial rotation-rolling, which reproduces the engagement of the imaginary wheel with the blank. With each elementary change of the tool's position in space with respect to the blank, a part of the metal is removed. As a result, the shape of the teeth flanks of the processed wheel, it is obtained the wrap of the family of the consecutive positions of the profile generator contour of the rotating tool relative to the blank.

The tool holder device shown in figure 11, (a) is adjusted to the grinding machines of the models: 5K32P53, 5330P, 53A50, 5A60, 5342.

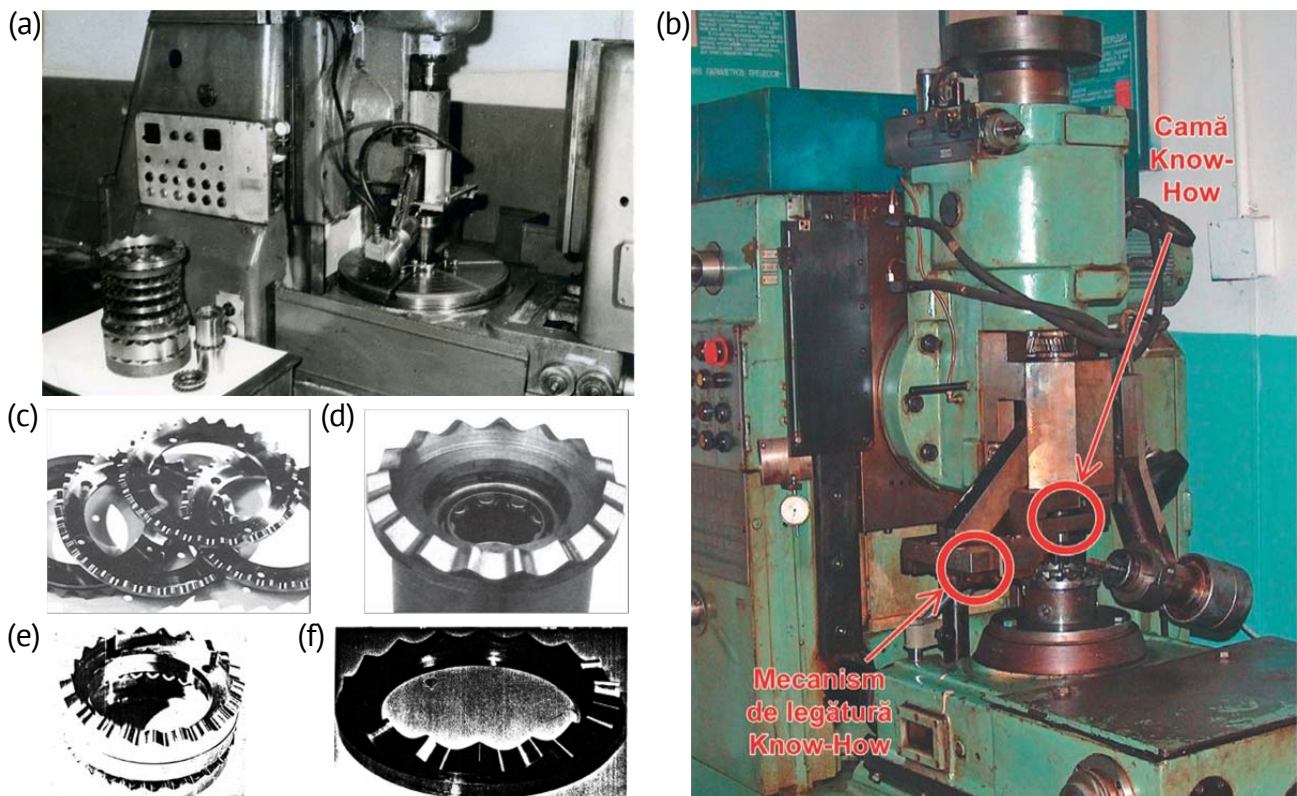


Figure 11. Machine-tool with teeth generation device with the tool in the shape of a truncated cone for generating the gear teeth by milling (a), rectification (b) and samples of manufactured toothed wheels by rectification for transmissions with reducer (c), (d), (e) and multiplier (f) regime.

8. Recommendations and constraints on TPD design

The TPD design with pre-set gear performance is achieved in the following succession:

1. According to the transmission report i stipulated in the design specification, the kinematic structure of the transmission $2K-H$, $K-H-V$ is identified or combined and the co-

ratio of the number of teeth for the gears Z_1 - Z_2 , and where appropriate Z_3 - Z_4 , is preventively chosen.

2. Depending on the constructive, kinematic and dynamic requirements, including load bearing capacity, compaction, mass and gauge, the configuration parameters $[Z_g-\theta;\pm 1]$ are preventively chosen.

3. According to the parametric equations of analytical description of the convex-concave profile of the teeth (6), the profilograms of the teeth in contact are designed.

4. Based on the analysis of the teeth profilograms and the parametric configuration $[Z_g-\theta;\pm 1]$ there are calculated:

- the reference gear multiplicity ε , %;
- the difference in curvature of the teeth flank profiles of the central wheel ρ_i according to (7) and of the satellite r in the contact points (ρ_i-r) ;
- the relative sliding of the teeth flanks conjugated in the contact points V_{sl} according to (16) and (20);
- effective contact tension σ_H considering the sliding in the contact.

5. Based on the analysis of load bearing capacity characteristics of the contact calculated in p. 4 (ε , $R-r$, S_E , σ_H) the configuration parameters are changed $[Z_g-\theta;\pm 1]$ and according to p. 3 a new contact geometry is reprojected to pursue the goal of obtaining:

- the minimum difference in curvature of the conjugate profiles (ρ_i-r) ;
- minimal sliding of the teeth flanks in contact (S_E) according to (21 and 22);
- the minimum profile angle of the teeth of the central wheel (α_w) (to reduce the load of the crank shaft bearings and the satellite wheel), etc.

Taking into account the conditions for minimizing the relative sliding in the contact of the flanks of the teeth S_E , of the difference in the teeth flank curves in contact (ρ_i-r) mm and of the profile angle of the teeth α_w :

- the configuration of the geometric parameters of the gears (δ , θ , β and Z) is identified, which would ensure optimal reference multiplicity ε (2-3 pairs of teeth);
- the configuration of the geometric parameters (δ , θ , β and Z) of the gear is identified, which would ensure $\alpha_w < 30^\circ$;
- the height of the teeth of the satellite wheel and the central wheel is modified (through shortening) so that we obtain the minimum allowable ratio of the relative sliding in the contact of the gear teeth.

In order to diminish (exclude) the relative sliding S_E between the active flanks of the conjugated teeth with convex-concave contact, the gear teeth are executed at an angle of inclination, so that by reducing the multiplicity of the reference gear ε to ensure optimal co-rotation between the front and the longitudinal teeth covering.

Figure 12, (a) shows the precession node with complementary assembly with the electric motor. The overall design of the precessional gearmotor with toothed wheels of the $2K-H$ type with circular arc – concave contact of the teeth. The satellite wheel 1 has two lateral crowns with the teeth 2 and 3 with circular arc profile and forms a whole in the shape of a conical cupola with the crank shaft 4. The teeth of the crown 2 of the satellite wheel 1 engage with the teeth of the immobile central wheel 5 mounted in the casing 6, and the teeth of the crown 3 engage with the teeth of the mobile central wheel 7 mounted on the drive shaft 8. The teeth of the central wheels 5 and 7 have concave profile described with the parametric equations (6).

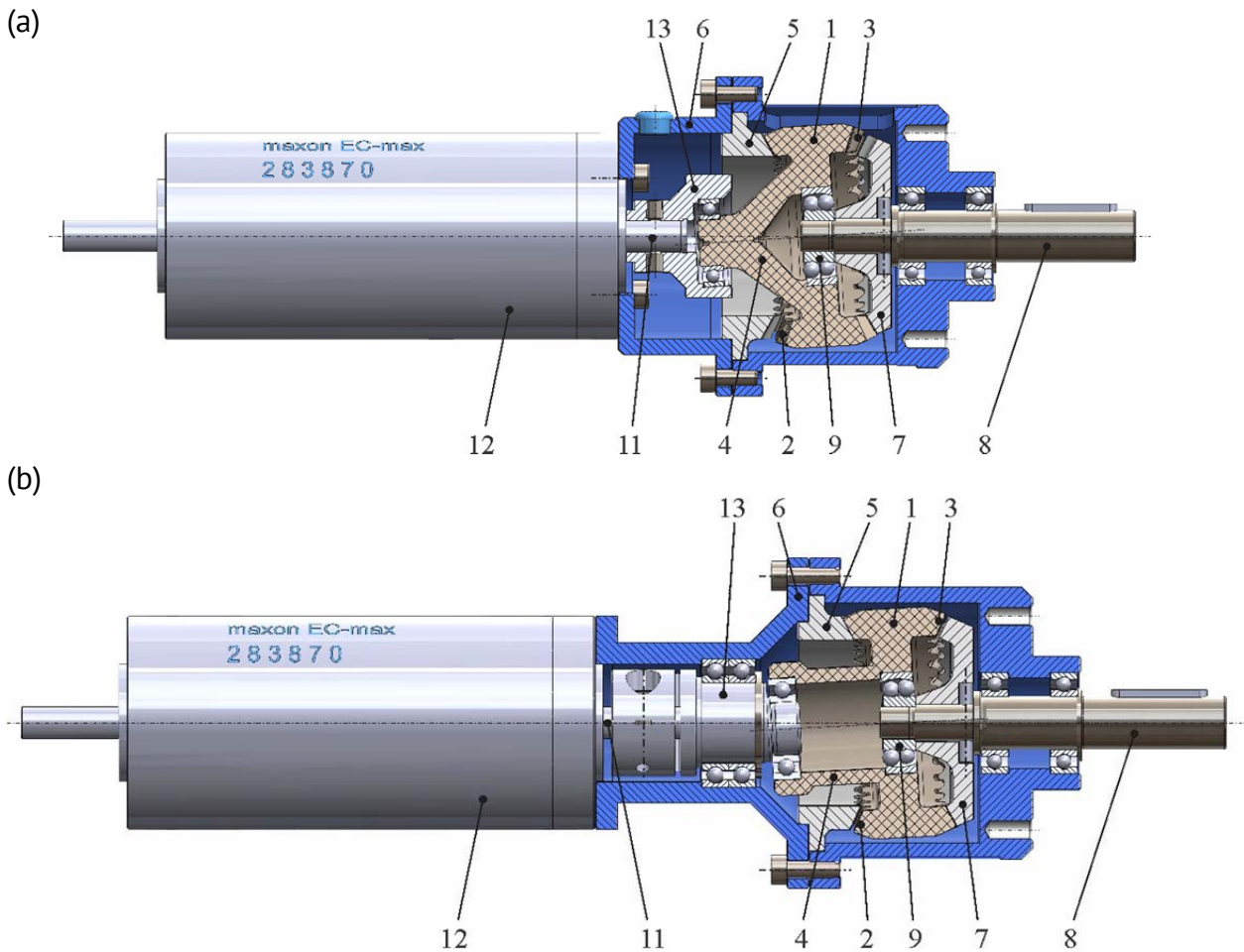


Figure 12. Precessional gearmotors with convex-concave gear of the teeth with the crank shaft in the shape of a conical cupola, $i=-124$ (a) and with the crank shaft in the tubular form, $i=-90$ (b).



Figure 13. A series of kinematic precessional reducers with gears with convex-concave contact of the teeth (a) and submersible precessional power-reducer (b).

The satellite wheel 1 is installed on the spherical ball bearing 9 located in the crank shaft cavity 4 in the precession center area O and supported on the end of the driven shaft 8. At the other end, the crank shaft 4 is installed in the bearing 10 mounted on the shaft 11 of the electric motor 12 via the eccentric 13.

When rotating the shaft 11 of the electromotor 12, the rotation movement by means of the eccentric 13 and the bearing 10 turns into the sphero-spatial movement of the

satellite wheel 1, thereby requiring the teeth of the conjugated wheels to engage and achieve the reduction of rotation with the transmission ratio.

$$i = -\frac{Z_2 Z_4}{Z_1 Z_3 - Z_2 Z_4} \quad 28$$

In the precessional gearmotor presented in figure 12, (b), the rotation movement of the shaft 11 of the electric motor 12 is transformed into the sphero-spatial motion of the satellite 1 by means of the bearing 14 mounted in the extension cavity of tubular form of the satellite 1 which fulfills the function of the crank shaft. The bearing 14 is mounted on the end of the eccentric 15 located at an angle θ to the axis of the shaft 11 of the electric motor 12. The eccentric 15 is in turn mounted on the bearings 16 and 17 in the housing 18 of the reducer.

In the gearmotor in figure 12, (a), the electric motor and the precessional reducer form an interdependent complementary structure, but in the gearmotor in figure 12, (b), the precessional reducer is an independent individual structure that can be coupled to different electric motors, modifying only the coupling cap.

Figure 13, (a) shows a series of kinematic precessional reducers with gears with convex-concave contact of the teeth. Figure 13, (b) shows the precessional power reducer with gears with convex / concave profile of the teeth of the central wheels designed for submersible special technique with the following feature:

Power, kW	6;
Torque, Nm	2950;
Gear ratio	- 144;
Efficiency	0.82;
Specific consumption of materials, kg/Nm	0.049;
Acoustic power level, dBa	60...75.

Remark 5: The geometry of teeth contact in the precessional gear is optimized by selective design from the perspective of gaining concrete advantages. The analysis of the projected profilogram looks like the profile angle of the teeth $\alpha_w = 42^\circ$, $\alpha_w > 30^\circ$ which results in increased reactions in the bearings of the crank shaft 4 and the satellite wheel 1. At the same time, from the analysis of the configuration parameters influence $[Z_g - \theta, \pm 1]$ it is found that the angle θ has the greatest influence on the profile angle α_w .

Remark 6: Based on the analysis of the defining characteristics of the load bearing capacity of the contact, namely the multiplicity of the reference gear ε %, of the difference in curvature of the conjugated profiles $(R - r)$ mm, of the relative sliding of the profiles in the contact S_E mm and effective contact tensions σ_{HE} by repeatedly designing the profilograms of the conjugated teeth the value configuration of the parameters δ , θ , r and z is identified for which we get minimum values for ε %, $(R - r)$ mm; S_E , α_w and σ_{HE} .

References

1. E. Wildhaber. Helical gearing. U.S. Patent nr. 1.601.750. (1926)
2. M. L. Novikov. Tooth gearings and also cam mechanisms with the dot system of gearing. Author's certificates of the USSR Nr. 109113. (1956) (in Russian)
3. S. P. Radzevich. High-conformal gearing: A new look at the concept of Novikov gearing. In: Proceedings of International Conference on Gears, October 5-7, 2015, Technical University of Munich. Garching, Germany, pp. 1303-1314. (2015)

4. I. A. Bostan. Establishment of planetary precessional transmissions with multi-pair gearing. Doctoral dissertation (Dr. Hab.), Moscow State Technical University of N. Bauman. Moscow. Volume 1, 511 p., Volume 2 (Annexes) 236 p. (1989) (in Russian)
5. I. A. Bostan. Precessional transmissions with multi-pair gearing. Chisinau, Stiinta, 356 p. ISBN: 5-376-01005-08. (1991) (in Russian)
6. I. A. Bostan. Precession tooth gearing. SU 1455094 A1. MKI F 16 H 1/32. B.I. Nr. 4. (1989) (in Russian)
7. I. A. Bostan. Gearing for precessional transmissions. Chisinau, Stiinta, 146 p. ISBN: 5-376-004848. (1988) (in Russian)
8. I. Bostan, V. Dulgheru, C. Glușco, S. Mazuru, M. Vaculenco. Anthology of Inventions. Vol. 2. Precessional Planetary Transmissions: The theory of generating of precession gears, dimensional control, computer aided design, industrial applications, descriptions of the invention. (Monography). Chisinau, Bons Offices. 542 p. ISBN 978-9975-80-283-3. (2011) (in Romanian)
9. V. Bostan. Mathematical models in Engineering. (Monography). Chisinau, Bons Offices, 470 p., ISBN 978, 9975-80-831-6. (2014) (in Romanian)
10. Patent. I. Bostan, I. Babaian. Manufacturing procedure of the profile modified teeth of precessional gears. S.U. 1663875 A1.MCI B23 F9/06. (1988) (in Russian)